



Hydrochemical characteristics, trace element sources, and health risk assessment of surface waters in the Amu Darya Basin of Uzbekistan, arid Central Asia

Shuie Zhan^{1,3} · Jinglu Wu^{1,2} · Miao Jin^{1,3}

Received: 12 March 2021 / Accepted: 30 July 2021 / Published online: 21 August 2021

© The Author(s), under exclusive licence to Springer-Verlag GmbH Germany, part of Springer Nature 2021

Abstract

Thorough knowledge of hydrochemical characteristics and trace element concentrations in surface waters is crucial for protection of this resource, especially in arid regions. Uzbekistan lies in central, arid Central Asia, and is experiencing severe water scarcity as a consequence of warming climate and accelerated human impacts. Fifty-five surface water samples were collected from the Amu Darya Basin of Uzbekistan (ADBU) and measured for relevant variables, to determine hydrochemical characteristics and evaluate water quality. River water samples from the middle reach and Amu Darya Delta (ADD) were dominantly $\text{HCO}_3\text{-Ca}$ and $\text{SO}_4\text{-Ca}\cdot\text{Mg}$ types, respectively, whereas water samples collected near the former shoreline and sewage outlets in the ADD were predominantly $\text{Cl-Ca}\cdot\text{Mg}$ and Cl-Na types, consistent with the distribution of sites that display high concentrations of trace elements and are seriously affected by human activities. Principal component analysis indicated that Pb and Cd in surface waters of the ADBU had industrial origins. Local agricultural activities are thought to have contributed to the concentrations of NO_3 , Zn, Ni, Hg, and Mn, through pesticide and fertilizer applications, and concentrations of Cu, Cr, As, and Co are controlled by mixed natural and anthropogenic sources. Water quality and health risk assessments indicated that unsuitable drinking waters are distributed mainly near the former shoreline and sewage outlets in the ADD, making human health risks in these areas high.

Keywords Trace elements · Hydrochemistry · Health risk · Former shoreline · Amu Darya Delta

Introduction

Water resources are important for socio-economic development and to sustain the natural environment (Graham et al. 2020). In arid Central Asia, water is the most critical factor driving social and economic development. Because of rapid population growth and climate change, however, water resources in Central Asia have been stressed beyond their natural limits, creating a suite of environmental and socio-

economic issues, including water quality deterioration, soil salinization, and consequent food crises (Jalilov et al. 2018). This is especially true in Uzbekistan, the most populous country in Central Asia, which receives an extremely limited amount of water from its upstream neighbors via shared rivers, making it impossible for the country to meet its residential, industrial, and agricultural water needs (Kundzewicz and Kowalczak 2009). In recent decades, the growing population, coupled with increasing agricultural irrigation and other water extraction in upstream regions, has led to several problems in Uzbekistan, including disappearance of some terminal lakes. The Aral Sea, once the fourth-largest inland water body in the world, has shrunk dramatically, from 68,478 km² in 1960, to 8,321 km² in 2018, exerting a huge impact on the local environment, especially on the Amu Darya Delta (Yang et al. 2020). As a result of the reduction in water volume, deterioration of water quality, and emission of pollutants, the health status of residents in the region has declined precipitously, expressed by high infant mortality rates, slower growth, and higher rates of morbidity. This is considered an ecological disaster (Micklin 2007; Schiermeier 2001), and water-related

Responsible Editor: Xianliang Yi

✉ Jinglu Wu
w.jinglu@niglas.ac.cn

¹ State Key Laboratory of Lake Science and Environment, Nanjing Institute of Geography and Limnology, Chinese Academy of Sciences (CAS), Nanjing 210008, China

² Research Center for Ecology and Environment of Central Asia, Chinese Academy of Sciences, Urumqi 830011, China

³ University of Chinese Academy of Sciences, Beijing 100049, China

environmental problems have become increasingly prominent in the basin (Crosa et al. 2006; Papa et al. 2004; Tornqvist et al. 2011).

The hydrochemistry of surface waters reflects the climate and environment of the watershed. The chemical composition of the water can be used to assess water quality and evaluate its potential for different uses (Ren et al. 2021; Rezaei et al. 2020; Wu et al. 2020). With this in mind, the many factors that control river hydrochemistry (e.g., local geology, hydrology, human activities) have been studied extensively in recent years (Han and Liu 2004). Those investigations found that trace elements in the aquatic environment are released mainly from natural sources, but also from human-mediated industrial, agricultural, domestic, municipal landfill, and mining activities (Li et al. 2018; Njuguna et al. 2020; Wang et al. 2017). High concentrations of trace elements in the aquatic environment pose potential risks. Multivariate statistical analyses, including principal component analysis (PCA), Pearson correlation analysis (CA), hierarchical cluster analysis (HACA), and discriminant analysis (CDA), have been used to explore the sources of pollutants (Wang et al. 2017; Zhan et al. 2020). Trace element contamination has often been quantified through indices such as the sodium sorption ratio (SAR), water quality index (WQI), or health risk index (HI) (Njuguna et al. 2020; Wei et al. 2021; Wu et al. 2020). Trace elements are important indicators of environmental change. Numerous studies have been carried out on concentrations, distributions, and sources of trace elements in the world's lotic systems, such as the Huai (Wang et al. 2017) and Tana Rivers (Njuguna et al. 2020). Studies of river hydrochemistry and trace elements can provide an effective basis to ensure the safety of water and protect water resources.

As the most important water resource in Uzbekistan and the Aral Sea Basin, the downstream aquatic environment of Amu Darya has always been the focus of research (Papa et al. 2004; Tornqvist et al. 2011). Few studies in this region, however, have incorporated measurement of both general hydrochemistry and trace elements, which creates great uncertainty for water resource management in Uzbekistan. To fill the aforementioned knowledge gaps, we conducted a preliminary study of surface waters in the Amu Darya Basin of Uzbekistan (ADBU) that aimed to (1) measure concentrations of major ions and trace elements in surface waters and assess variations in their spatial distributions; (2) identify probable sources and factors that influence trace element concentrations, and multiple statistical approaches; and (3) evaluate the suitability of surface water for different applications, as well as potential threats to human health, based on trace elements and hydrochemical indicators.

Materials and methods

Study area

Uzbekistan is located in Central Asia, between 37° and 45°N latitude and 56° and 73°E longitude (Fig. 1). It is completely landlocked, and lowland plains account for 80% of the area, most of which are located in the Kyzylkum Desert, in the northwest. The climate of Uzbekistan is continental, with high inter-seasonal differences in air temperature and rainfall. Precipitation falls mainly during winter and spring, with mean annual values ranging from 80 to 200 mm year⁻¹ in the desert plain areas and 600 to 800 mm year⁻¹ in the mountainous plateau areas. Water resources of the country are provisioned mostly by surface runoff to the Amu Darya and Syr Darya Rivers, which drain into the Aral Sea (Mirshadiev et al. 2018; UENP 2016). The Amu Darya has a total length of 2,550 km and originates in the Pamir Mountains, known as the “Water Tower of Central Asia.” The Zeravshan River (ZR) flows into the middle reach of the Amu Darya, which ultimately empties into the Aral Sea through an extensive delta (Wang et al. 2016). The main sources of recharge in the basin are snow and glacial meltwaters, with highest flows occurring in July and August. Groundwater recharge also plays an important role, often exceeding 30% of annual runoff (Awan et al. 2015). Because of large-scale expansion of irrigation systems and climate warming, average discharge of the Amu Darya into the Aral Sea has declined from 78 to 0–1 km³ year⁻¹, leading to many ecological problems in the region (Yang et al. 2020). The most important problem is the drying of the Aral Sea and consequent collapse of the local ecological environment surrounding the lake, a process that is particularly severe in the lower Amu Darya, and led to the area being declared a World Disaster Zone in 1991 (Crosa et al. 2006).

The Amu Darya Delta (ADD) lies on the lower Amu Darya, at the southern edge of the Aral Sea (Fig. 1). The region covers an area of 6.3×10^4 km² and has a population of more than 3 million people, of whom approximately 70% are engaged in crop production, animal husbandry, and horticulture (Dubovyk et al. 2013; Papa et al. 2004). The delta has an extreme continental climate. Temperature ranges from 45 to -30°C, with an annual average of approximately 13°C. Average precipitation is less than 100 mm year⁻¹, and potential evaporation exceeds 1000 mm year⁻¹ (Jarsjo et al. 2017). Therefore, the region depends almost entirely on upstream runoff waters that flow through rivers and canals, and are used for agricultural irrigation and domestic purposes. Over the past few decades, however, the Amu Darya has gone dry before reaching the former shoreline of the Aral Sea (Tornqvist et al. 2011). Therefore, the ADD region has become one of the most sensitive and ecologically fragile areas of Uzbekistan, because of its low precipitation, high evaporation, and ever-expanding human activities.

Fig. 1 Location of the study area and sampling sites (see Fig. S2 for sampling locations along the ADD)



The entire study area consists mainly of sedimentary, extrusive, and metamorphic rocks that formed during the Paleogene to Quaternary (Fig. S1). The ADD itself is composed primarily of alluvial and lacustrine sediments, with the alluvial deposits functioning as a shallow aquifer. Under the evaporative conditions on the delta, gypsum, halite, and substantial amounts of calcite were deposited (Schettler et al. 2013). Groundwater flow on the ADD is dominated largely by morphology. Because of the shrinking size of the Aral Sea, the shoreline has been displaced, blocking inflow of seawater into the aquifer and its subsequent return to the lake, which has led to a decline in groundwater level and an increase in salinity (Shibuo et al. 2006).

Sample collection and analysis

In August 2019, a field survey was conducted across the ADBU that covered its main regions, including the ADD and ZR (Fig. 1). Fifty-five water samples (including river water, ditch water, and drainage water) were collected at a depth of approximately 30 cm below the water surface. The geographic locations of each sampling site were recorded with a portable GPS. Each water sample was filtered immediately through a 0.45-µm Millipore nitrocellulose filter (Merck-Millipore) and then divided into two parts, one for anion analysis, and another that was acidified with ultra-pure HNO₃ to a pH < 2 for cation and trace element analysis. Prior to laboratory analysis, all collected water samples were refrigerated at approximately 4°C.

At the same time that water samples were collected, pH and total dissolved solids (TDS) were measured using a multi-parameter YSI 6500 water quality analyzer (USA).

Carbonate (HCO₃⁻) alkalinity was measured by titration using HCl and methyl orange indicator, as soon as possible after water sampling in the field. NO₃-N was determined using a model CFA-San plus continuous flow analyzer (SKALAR, Netherlands), with a detection limit of 0.01 mg/L. Major cations (K⁺, Na⁺, Ca²⁺, and Mg²⁺) were determined by inductively coupled plasma mass spectrometry, using an ICP-OES (Prodigy, USA) with detection limits of 0.1 mg/L for K⁺, 0.03 mg/L for Na⁺, 0.01 mg/L for Ca²⁺, and 0.003 mg/L for Mg²⁺. Additionally, anions (SO₄²⁻ and Cl⁻) were determined by ion chromatography, with an ICS-2000 (Dionex Corporation, USA). Detection limits for Cl⁻ and SO₄²⁻ were 0.18 and 0.05 mg/L, respectively. To assess analytical quality, reagent blanks were run alongside sample analyses. All values for tested blanks were < 5% of the sample values. Measured values for standard solutions were all within the acceptable range of 93.2–108.6%. Relative standard deviations (RSD) of replicates were all within 10.3%.

Concentrations of trace elements were analyzed using an ICP-MS 7700x (PerkinElmer Inc., USA) under optimum analytical conditions. After initial calibration, a standard was run after every 10 samples to test data accuracy. Based on their toxicities and potential environmental risks from the perspective of water pollution, as well as their widespread distribution in recent years, trace elements investigated in this study were copper (Cu), zinc (Zn), manganese (Mn), cadmium (Cd), chromium (Cr), cobalt (Co), nickel (Ni), lead (Pb), mercury (Hg), and arsenic (As), and their detection limits were 0.01, 0.1, 0.02, 0.005, 0.05, 0.005, 0.03, 0.01, 0.02, and 0.05 µg/L, respectively. Measured values in standard solutions were in the range of 91.6–105.3%. The RSD of replicates for all trace elements was below 10%.

Water quality assessment

The water quality index (WQI) reflects the combined impact of multiple water quality variables, and is considered to be a powerful tool that presents a comprehensive picture of water quality in the study area (Rezaei et al. 2019; Wei et al. 2021). It is calculated as follows:

$$WQI = \sum \left[W_i \times \left(\frac{C_i}{S_i} \right) \right] \times 100 \quad (1)$$

where W_i represents the weight of each variable i and the relative importance of each variable used to assess drinking water quality, summarized in the supplementary materials (Table S1). It is calculated according to the eigenvalues of each principal component and the factor loading of each variable in a principal component analysis of all physico-chemical variables (Wang et al. 2017). C_i is the measured concentration of elements or ions in water samples, and S_i is the World Health Organization (WHO) guideline concentration for each element or ion (WHO 2011). Accordingly, water quality can be divided into five classes: excellent ($0 \leq WQI < 50$); good ($50 \leq WQI < 100$); medium ($100 \leq WQI < 200$); poor ($200 \leq WQI < 300$); and very poor ($WQI \geq 300$).

Health risk assessment

Human health risks associated with specific chemicals were considered primarily from the perspective of non-carcinogenic risks. Direct ingestion and dermal absorption are the two primary modes of trace element exposure from water sources, so they are usually considered when assessing health risks of trace elements (Islam et al. 2020). According to the risk guidelines of the USEPA (USEPA 2004), the exposure dose for direct ingestion ($ADD_{\text{ingestion}}$) and dermal absorption (ADD_{dermal}) were calculated as follows:

$$ADD_{\text{ingestion}} = \frac{C_w \times IR \times EF \times ED}{BW \times AT} \quad (2)$$

$$ADD_{\text{dermal}} = \frac{C_w \times SA \times K_p \times EF \times ET \times ED \times 10^{-3}}{BW \times AT} \quad (3)$$

where C_w is the concentration of trace elements in water samples ($\mu\text{g/L}$); IR is the ingestion rate (L/day); EF is the exposure frequency (days/year); ED is the exposure duration (years); BW is the body weight (kg); AT is the average time for non-carcinogens (days); SA is the exposed skin area (cm^2); K_p is the dermal permeability coefficient in the samples (cm/h); and ET is the exposure time (h/day). Specific values of the parameters are given in Table S2.

The potential non-carcinogenic risks were assessed by the hazard quotient (HQ). The total potential non-carcinogenic risks caused by two different pathways were expressed as a hazard index (HI), which was defined as:

$$\text{Hazard Quotient}(HQ) = ADD/RfD \quad (4)$$

$$\text{Hazard Index}(HI) = \sum (HQ_{\text{ingestion}} + HQ_{\text{dermal}}) \quad (5)$$

where RfD is the reference dose ($\mu\text{g/kg/day}$), $RfD_{\text{dermal}} = RfD_{\text{ingestion}} \times ABS_g$, and ABS_g is the gastrointestinal absorption factor (dimensionless) (Table S2). $HQ_{\text{ingestion}}$ is the hazard quotient from direct ingestion and HQ_{dermal} is the hazard quotient from dermal absorption. When values of HQ are > 1 , non-carcinogenic effects should be considered. Similarly, an $HI < 1$ indicates that the measured element has a small adverse health impact on local residents, and an $HI \geq 1$ indicates a greater likelihood of an adverse health impact.

Statistical analyses

On the basis of hydrochemistry and trace elements, water samples were classified into different types, controlled by natural and/or human processes, using HACA, which were then plotted with SPSS 25.0. In addition, in combination with hydrochemistry, sources of trace elements in surface water were identified by PCA, which was performed using SPSS 25.0 and Canoco 5.0. ArcGIS 10.2 software was used to visualize the WQI and HI outcomes and display their spatial distributions.

Results and discussion

Spatial patterns of chemical variables in surface waters

Surface water showed slightly alkaline characteristics, with pH values of 8.12 ± 0.15 and 7.90 ± 0.46 in the ZR and ADD, respectively (Table 1). Differences in TDS of water samples may be related to the patterns and intensity of human activities and consequent pollution (Han and Liu 2004). Surface water in the ADD had an average TDS value 3,800 mg/L, ranging from 242 to 119,827 mg/L, which is larger than the mean value (283 mg/L) for large rivers worldwide (Gaillardet et al. 1999). The ZR water had a lower average TDS value (322 mg/L). Highest TDS values for the ADD and ZR regions were found at sample sites S10 (119,827 mg/L) and S48 (865 mg/L), which were located near a textile factory and farmland, respectively. In contrast, river water near the mountain pass in the ZR has the lowest TDS values.

A statistical analysis of hydrochemical variables revealed that the order of cation abundances in the ZR was $\text{Ca}^{2+} > \text{Na}^+ > \text{Mg}^{2+} > \text{K}^+$. Concentrations of Ca^{2+} and Na^+ ranged from 34.91 to 104.37 mg/L and 2.26 to 92.10 mg/L, with average values of 55.86 mg/L and 28.01 mg/L, respectively. Mean concentrations of Mg^{2+} and K^+ were 14.74 mg/L and 2.98 mg/L, respectively (Table 1). For the ADD water, the

Table 1 Statistical analysis of hydrochemical variables and trace element concentrations in 55 surface water samples across the ADBU

Variable	ADD				ZR				WHO Standards	World average
	Min	Max	Ave	SD	Min	Max	Ave	SD		
pH	6.64	8.55	7.90	0.46	7.96	8.35	8.12	0.15	6.5-8.5 ^a	–
TDS (mg/L)	242	119,827	3,800	17,193	94	865	322	256	1,000 ^a	283 ^c
Ca ²⁺ (mg/L)	51.50	664	152	129	34.91	104.37	55.86	28.09	200 ^a	30.26 ^c
K ⁺ (mg/L)	2.88	1,440	39.36	207	2.04	4.34	2.98	0.85	–	3.48 ^c
Mg ²⁺ (mg/L)	10.59	14,303	374	2,056	4.92	31.90	14.74	9.98	150 ^a	34.64 ^c
Na ⁺ (mg/L)	32.93	56,949	1,442	8,190	2.26	92.10	28.01	35.83	200 ^a	11.41 ^c
Cl ⁻ (mg/L)	1.77	71,314	1,714	10,272	1.02	77.32	22.99	31.28	250 ^a	48.60 ^c
SO ₄ ²⁻ (mg/L)	77.62	54,268	1,508	7,798	37.18	325.97	115.12	113.52	250 ^a	37.58 ^c
HCO ₃ ⁻ (mg/L)	67.05	872	175	127	135.60	228.83	182.19	31.50	250 ^a	110.61 ^c
NO ₃ -N (mg/L)	0.02	59.43	1.43	8.55	0.02	1.19	0.62	0.36	11.0 ^a	–
Cu (µg/L)	0.61	29.82	1.91	4.14	0.17	1.25	0.51	0.44	2000 ^a	1.48 ^d
Zn (µg/L)	9.60	82.87	22.55	12.28	14.08	34.61	24.14	7.50	5000 ^b	0.60 ^d
Mn (µg/L)	0.42	839.54	54.67	159.08	0.69	6.70	3.17	2.59	400 ^a	34.0 ^d
Cd (µg/L)	0.00	1.50	0.06	0.22	0.01	0.05	0.02	0.02	3 ^a	0.080 ^d
Cr (µg/L)	0.75	5.54	1.03	0.68	0.87	1.60	1.20	0.26	50 ^a	0.70 ^d
Co (µg/L)	0.03	5.72	0.39	0.94	0.04	0.11	0.07	0.03	50 ^a	0.148 ^d
Ni (µg/L)	0.25	11.81	0.98	1.73	0.36	0.61	0.45	0.09	70 ^a	0.80 ^d
Pb (µg/L)	0.12	2.25	0.27	0.35	0.12	0.23	0.17	0.04	10 ^a	0.079 ^d
Hg (µg/L)	n.a	0.19	0.03	0.03	n.a	0.02	0.01	0.01	6 ^a	–
As (µg/L)	0.75	87.18	5.55	12.28	0.62	1.80	1.29	0.42	10 ^a	0.62 ^d

^a WHO drinking water guidelines (WHO 2011)

^b USEPA drinking water standards (USEPA 2010)

^c Gaillardet et al. (1999)

^d Gaillardet et al. (2005)

abundances of cations were ordered as follows: Na⁺ > Ca²⁺ > Mg²⁺ > K⁺. Na⁺ and Ca²⁺ ranged from 32.93 to 56,949 mg/L and 51.50 to 664 mg/L, with average values of 1,442 mg/L and 152 mg/L, respectively. Mean concentrations of Mg²⁺ and K⁺ were 374 mg/L and 39.36 mg/L, respectively (Table 1). Na⁺ and Ca²⁺ were the predominant cations in the ADBU.

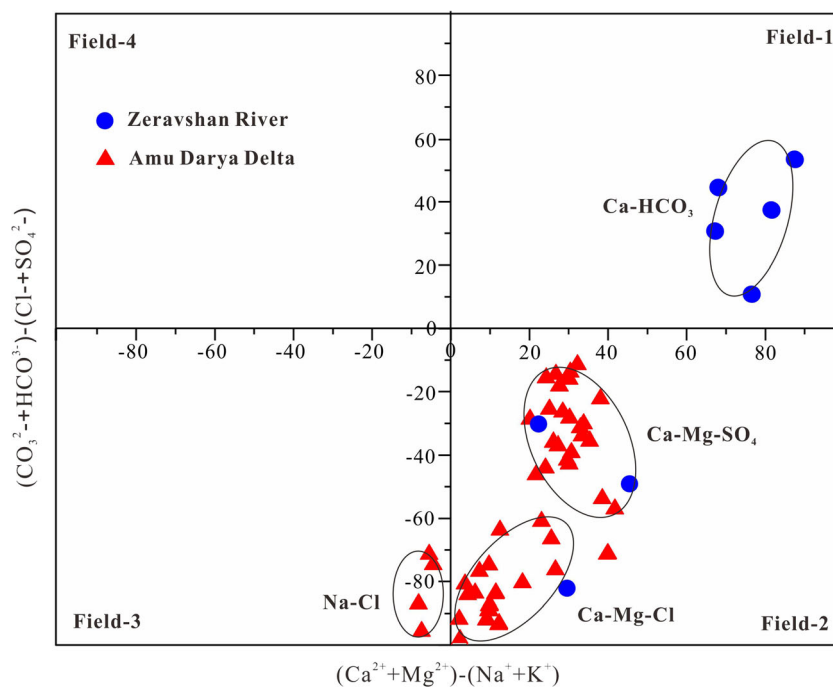
Anion concentrations were present in the order HCO₃⁻ > SO₄²⁻ > Cl⁻ in the ZR water. The HCO₃⁻ concentration ranged from 135.60 to 228.83 mg/L, with an average value of 182.19 mg/L. Concentrations of SO₄²⁻ and Cl⁻ ranged from 37.18 to 325.97 mg/L and 1.02 to 77.32 mg/L, with mean values of 115.12 mg/L and 22.99 mg/L, respectively (Table 1). For the ADD water, the order of abundance of anions was Cl⁻ > SO₄²⁻ > HCO₃⁻. Concentrations of SO₄²⁻ and Cl⁻ ranged from 77.62 to 54,268 mg/L and 1.77 to 71,314 mg/L, with average values of 1,508 mg/L and 1,714 mg/L, respectively. Concentrations of HCO₃⁻ ranged from 67.05 to 872 mg/L, with an average value of 175 mg/L (Table 1). HCO₃⁻ was the predominant anion in the ZR, whereas the water in the ADD was dominated by SO₄²⁻ and Cl⁻. In general, compared

with world averages, ion concentrations in the surface waters of the ADD are high (Gaillardet et al. 1999).

Hydrochemistry of surface waters

A Chadha diagram was used to classify major hydrochemical types in the ADBU, and it elucidates the role of major ions, both cations and anions, in the chemistry of surface waters (Chadha 1999). The classification is based on relationships between alkaline earths (Ca²⁺ + Mg²⁺), alkali metals (Na⁺ + K⁺), weak acidic anions (CO₃²⁻ + HCO₃⁻), and strong acidic anions (Cl⁻ + SO₄²⁻). Four fields within the diagram, containing four different types of hydrochemical facies, were obtained (Fig. 2). In the study area, 49.1% (n=27) of the water samples were SO₄-Ca-Mg type, which are dominated by Ca²⁺ and SO₄²⁻. Two of these samples were collected from the ZR, whereas all the others were collected from the ADD (Fig. 2). Generally, high Ca²⁺ and Mg²⁺ concentrations occur through the dissolution of Fe-Mg minerals, such as pyroxene, amphibole, and biotite. Alternatively, dissolution of carbonates may also have contributed these ions to surface water.

Fig. 2 Chadha diagram, illustrating the hydrochemical classes of surface waters in the ADBU



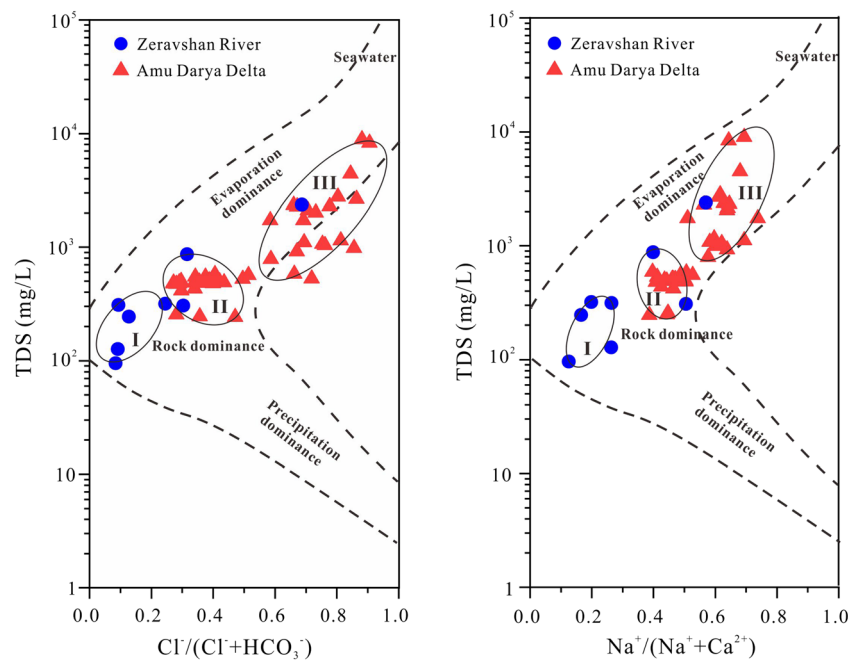
High values of Ca^{2+} and SO_4^{2-} are probably from the dissolution of gypsum (Schettler et al. 2013). Of the remaining samples, 9% ($n=5$) were $\text{HCO}_3\text{-Ca}$ type, formed by the reaction of rainwater containing CO_2 and CaCO_3 -bearing minerals in the recharge zones (Raj and Shaji 2017), and all these samples were from the ZR. Out of all the water samples, 34.5% ($n=19$) were in the Cl-Ca-Mg -type category, and 7% ($n=4$) were in the Cl-Na -type category. All these samples were from the ADD, with the exception of a single sample from the ZR. Higher Cl^- concentrations may be associated with local agricultural activities and domestic sewage discharge (Khanday et al. 2021). Widespread irrigated agriculture in the study area has led to abundant use of pesticides and organic fertilizers, which are now pollutants in local surface waters (Papa et al. 2004). Also, because of the geographic location of the study area, waters undergo high evaporative concentration, which also contributes to the high Cl^- concentrations in surface waters. The hydro-facies distribution showed that the hydrochemical types in the basin followed the order $\text{HCO}_3\text{-Ca} < (\text{Cl-Ca-Mg} + \text{Cl-Na}) < \text{SO}_4\text{-Ca-Mg}$, indicating the influence of human activities.

Mechanisms that control surface water chemistry

The chemical composition and characteristics of surface waters are generally controlled by natural processes (Gibbs 1970) and human activities (Ren et al. 2021; Gaillardet et al. 1999). The natural mechanisms that control surface water hydrochemistry can be inferred from the three end members in a Gibbs diagram (Fig. 3). Using a combination of the ratio of $\text{Na}/(\text{Na} + \text{Ca})$ and $\text{Cl}/(\text{Cl} + \text{HCO}_3)$, along with TDS in

water, Gibbs divided the plot into three domains: rock dominance, evaporation dominance, and precipitation dominance (Gibbs 1970). Waters in group III (Fig. 3) fell within the evaporation dominance zone and are characterized by high ratios of $\text{Na}/(\text{Na} + \text{Ca})$ and $\text{Cl}/(\text{Cl} + \text{HCO}_3)$, and high concentrations of TDS, suggesting that evaporative concentration is the primary control on the hydrochemistry. Waters in this group were mostly from the ADD, and their corresponding hydrochemical types were dominated by Ca-Mg-Cl and Na-Cl . Waters in group I fell in the rock dominance zone and are characterized by low ratios of $\text{Na}/(\text{Na} + \text{Ca})$ and $\text{Cl}/(\text{Cl} + \text{HCO}_3)$ and moderate concentrations of TDS, indicating the influence of rock weathering. These waters were collected near the mountain pass, and the corresponding hydrochemical type was Ca-HCO_3 . Group II waters represent an intermediate state, with moderate TDS concentrations and $\text{Na}/(\text{Na} + \text{Ca})$ and $\text{Cl}/(\text{Cl} + \text{HCO}_3)$ ratios, which indicates control by both rock weathering and evaporative concentration processes, and corresponds to a Ca-Mg-SO_4 type. Overall, the main natural mechanism that controls chemistry of surface water in the ZR is rock weathering. In the ADD, surface water chemistry is mainly dominated by rock weathering and evaporative concentration, associated with the arid climate of the study area. In some heavily polluted rivers, major element chemistry is dominated by human activities. Examples include the Elbe and Wisla Rivers, which are dominated by wastewater discharge from coal and salt mines (Gaillardet et al. 1999). Hence, we decided to further explore the sources of chemical elements in surface waters of the study area.

Fig. 3 Gibbs diagram showing the main natural processes that control hydrochemistry in the Zeravshan River and on the Amu Darya Delta



Spatial variability of trace element concentrations

Spatial heterogeneity of natural (background) element concentrations in different districts of the basin, as well as in the location of anthropogenic activities across the landscape, has led to heterogeneous distributions of trace elements in regional surface waters. In general, the variability in trace element concentrations in surface waters of the ADBU was high, especially for Mn and Zn, which had larger SD values than other elements (Table 1). According to their mean values, trace elements were divided into three categories, i.e., those with high abundance (> 20 µg/L), moderate abundance (1 to 20 µg/L), and low abundance (<1 µg/L). These three categories contained Mn and Zn; As and Cu; and Cr, Cd, Co, Ni, Pb, and Hg, respectively. With the exception of Zn and Cr, mean concentrations of trace elements in surface waters of the ADD were higher than those of the ZR (Table 1), reflecting the fact that concentrations of trace elements in most ADD water samples were higher than concentrations in samples from the ZR (Fig. 4). Among the samples, S10 had the highest concentrations of Cu, Cr, Co, and As; S02 had the highest concentrations of Zn, Ni, and Hg; S03 had the highest concentration of Mn; and S12 had the highest concentrations of Cd and Pb. Concentrations of Mn and As in some samples exceed the WHO guidelines, indicating that some waters in the ADD are polluted by trace elements.

Sample classification

HACA grouped samples by linking inter-sample similarities, and illustrates the overall similarity among variable in the dataset. Hierarchical agglomerative clustering by the average

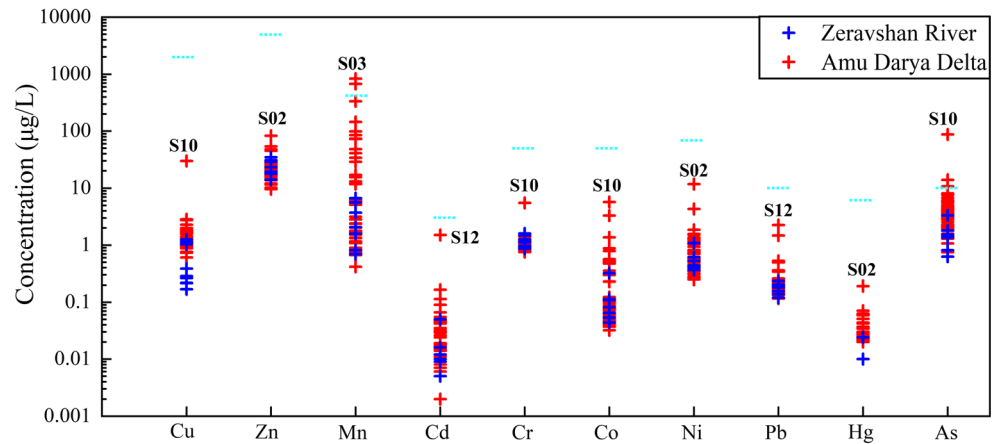
linkage method (between groups) was applied to physical and chemical variables for sample classification, which yielded a dendrogram with three statistically significant clusters at $(Dlink/Dmax) \times 100 < 15$. Clusters 1, 2, and 3 contained 5 (S51-S55), 27 (S14, S16-S17, S20-S25, S28-S31, S33-S35, S37-S38, S40, S42-S47, and S49-S50), and 23 (S01-S13, S15, S18-S19, S26-S27, S32, S36, S39, S41, and S48) water sampling sites, respectively (Fig. 5).

Samples in cluster 1 were all collected near the mountain pass in the ZR, whereas samples in cluster 2 were distributed across two regions (Fig. 1). Samples in these two groups were essentially obtained from river water, with relatively low concentrations of trace elements and TDS, indicating they are influenced primarily by natural processes. Cluster 1 is controlled mainly by rock weathering, whereas cluster 2 is controlled by both rock weathering and evaporative concentration processes, corresponding to HCO_3^-Ca type and SO_4^-CaMg type, respectively. Cluster 3 samples came mostly from sites near sewage outlets and the former shoreline in the ADD. In addition to being controlled by strong natural evaporation processes, samples in that cluster might be influenced by human activities. Waters in this group had relatively high abundances of Cl^- , trace elements, and TDS. Hydrochemical types were dominated by $Cl-CaMg$ and $Cl-Na$ types, and displayed characteristics distinct from those of the other two groups.

Source identification of trace elements

To identify the sources of trace elements in surface waters of the ADBU, we used SPSS and Canoco software to carry out PCA. The Kaiser-Meyer-Olkin (KMO) scores (0.823) and

Fig. 4 Trace element concentrations in surface waters of the ADBU. Note that concentrations are plotted on a log scale. Blue dotted line indicates the WHO drinking water standards (2011). The sampling site from which the highest concentration value was obtained is indicated for each element.



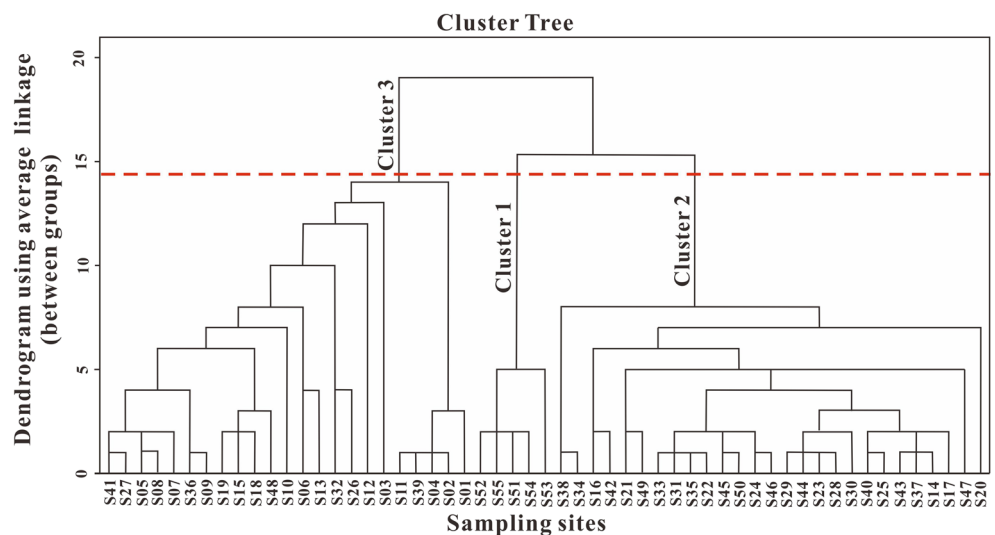
Bartlett's sphericity test values ($p = 0.000$) indicated that the datasets were appropriate for PCA. PCA extracted a total of two dimensions, which explained 89.10% of the variation in the distribution of chemical compositions (Fig. 6b). The 55 sampling sites were divided into four quadrants. Cluster 1 and cluster 2 were distributed in the second and third quadrants, which represented inputs from natural sources with negligible human influence. Cluster 3 was present mainly in the first and fourth quadrants, which probably indicated inputs from anthropogenic sources.

Three principal components explained 86.0% of the variance in the analyzed dataset (Fig. 6a), and were all distributed in the sampling sites of cluster 3 (Fig. 6b). TDS, Na^+ , Mg^{2+} , K^+ , SO_4^{2-} , Cl^- , HCO_3^- , Cu, Cr, As, and Co had high positive loadings in PC1, which explained 55.57% of the variance in the data matrix (Fig. 6a). PC1 was related to ions of naturally occurring salts and anthropogenic pollution sources. The salt ions in surface waters were produced primarily from various types of parent rock. Fertilizers and pesticides used in agriculture, along with household and municipal waste, also contributed ions (Khanday et al. 2021). Previous studies found that

high Cu, Cr, As, and Co concentrations in water are mainly attributable to anthropogenic sources, including domestic sewage, and agrochemical and industrial wastes (Habib et al. 2020; Islam et al. 2020). Spatially, sampling sites in PC1 are found in urban outfalls, near river mouths and the former shoreline of the ADD, and include S36, S15, S04, S05, S07, S48, S18, S19, and S10 (Fig. 6b). Of these, sample S48, which was collected near the textile factory outfall, had the highest concentrations of Cu, Cr, As, and Co in the study area. Sample S10 was located near farmland with the highest concentrations of As and Co in the ZR. The combination of TDS, Na^+ , Mg^{2+} , K^+ , SO_4^{2-} , Cl^- , Cu, Cr, As, and Co values reflect the overall influences of natural processes and human activities on water chemistry.

PC2 explained 21.03% of the variance, with strong positive loadings of NO_3^- , Zn, Ni, and Hg, and moderate loadings of Ca (0.66) and Mn (0.70) (Fig. 6a). It mostly included the S01-S03, S08, S11, S26-S27, S32, S39, and S41 sampling sites, which were located in drainage outlets of the irrigated farming area or near the former shoreline in the ADD region (Fig. 6b). High concentrations of NO_3^- , Zn, Ni, Hg, and Mn in the water

Fig. 5 Dendrogram based on agglomerative hierarchical clustering for water samples in the ADBU.



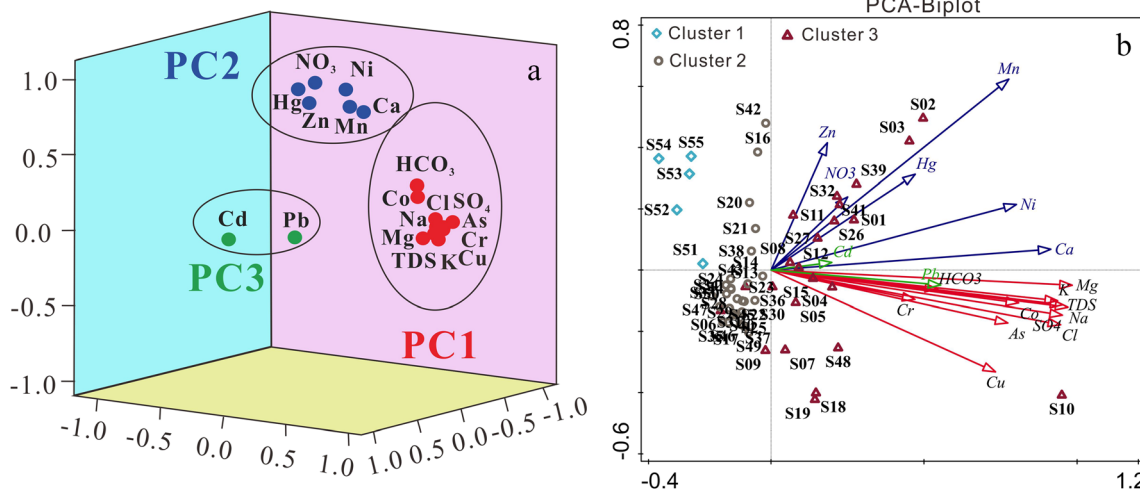


Fig. 6 Principal component analysis (PCA) for trace elements in surface waters in the ADBU. **a** Component plot in rotated space, using SPSS, and **b** loading plot in two dimensions, using Canoco.

samples may be related to the agricultural activities in this area (Chanpiwat and Sthiannopkao 2014). To increase crop yields, large amounts of nitrogen fertilizer and pesticides have been used in the ADD, resulting in the spread of toxic chemicals in the farmlands (Glantz 1999). In addition, NO₃ from nitrogen fertilizers is susceptible to loss through leaching, and contributes to surface-water and groundwater pollution in the area (Egamberdiyeva et al. 2001).

Cd and Pb exhibited high loadings in PC3, explaining 8.41% of the variance, but only occurred in S12, indicating that it may reflect a nearby point source of pollution (Fig. 6). Cd and Pb mainly originate from industries near the sampling point that produce textiles, leaded gasoline, and chemicals (Islam et al. 2020; Zeng et al. 2015).

Water quality and health risk assessment

Suitability for drinking purposes

Given that surface waters represent a major water resource for regional inhabitants, the WQI was applied to evaluate the potability of surface water in the ADBU. Calculated WQI values for water samples ranged from 7.87 to 195.85, with a mean of 35.91. The sample from S10 yielded an exceedingly high value (6706.7) and was excluded from calculation of the mean. Of the 55 water samples, two displayed very poor water quality, two had poor water quality, and two fell in the medium water quality range (Fig. 7). All were collected near the former shoreline and sewage outfalls in the ADD. Water from all other sites in the ADBU plotted in the good or excellent water categories, with WQI values < 100, indicating suitability for drinking. Overall, the surface water in the ADBU is in good condition, with only 12.6% of the samples unsuitable for drinking (WQI ≥ 100). Among all the water samples, 23.4%

of samples had good quality (0 ≤ WQI < 50), and 63.8% had excellent quality (50 ≤ WQI < 100). More attention, however, should be paid to sites near the former shoreline and sewage outfalls in the ADD, where water would require salinity and pollutant treatment to make it potable.

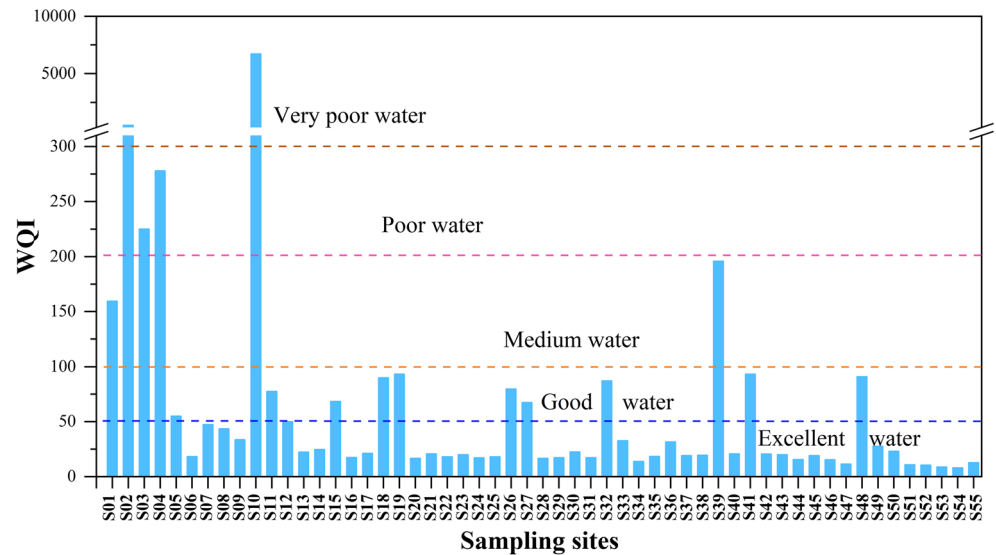
Human health risk assessment

We used the traditional risk assessment guidelines of the USEPA (2004) to evaluate the risk of trace elements in surface waters from the ADBU to human health. Table S3 presents the HQ and HI for direct ingestion and dermal pathways, as they relate to adults and children in the ZR and ADD regions.

In the ADD region, HQ_{ingestion} values of all elements, except As and Mn, are < 1, suggesting that these elements pose little hazard. However, maximum HQ_{ingestion} values for As (8.56 for adults and 8.92 for children) are > 1, and for Mn (1.03 for adults and 1.07 for children) are near 1, which implies that As and Mn may cause adverse, non-carcinogenic health effects. The HQ_{dermal} values for all the elements, for both adults and children, were < 1, indicating that these elements pose little hazard via dermal absorption. Average HI values, in decreasing order, were As > Mn > Co > Cr > Pb > Cd > Hg > Zn > Ni > Cu, suggesting that the greatest potential contributor to chronic risks was As, followed by Mn, whereas the lowest were Ni and Cu, for both adults and children.

In the ZR region, HQ_{ingestion} and HQ_{dermal} values for both age populations, with respect to all the elements, were below 1, the highest being for As, followed by Cr. In our study, HQ_{ingestion} and HQ_{dermal} values were larger for children than for adults, indicating that children are more vulnerable and exposed to health hazards from exposure to trace elements in water, in agreement with previous findings (Habib et al. 2020; Njuguna et al. 2020).

Fig. 7 Water quality assessment by WQI values of surface water in the ADBU



Spatial variations in water quality values and health risk assessments (HI values for adults) in the ADD are shown in Fig. 8. Highest WQI values occurred near the former shoreline, indicating that the shoreline zone has the worst water quality throughout the whole ADBU (Fig. 8a; Fig. S2). Similarly, highest values of HI also occurred near the former shoreline, where the most serious trace element pollution occurs. HI values for As, Mn, Co, Hg, Cu, Cr, and Zn were

consistent with WQI results. Waters with the highest values were found near the former shoreline, followed by samples taken near the outfalls around the city of Nukus (Fig. 8a–h). Highest HI values for Cd, Pb, and Ni were calculated for samples that came from near the former shoreline (Fig. 8i–k). Discharge waters from irrigated lands and industrial wastewater possess large amounts of salts, pesticides, and toxic elements, which get carried downstream in the basin (Crosa

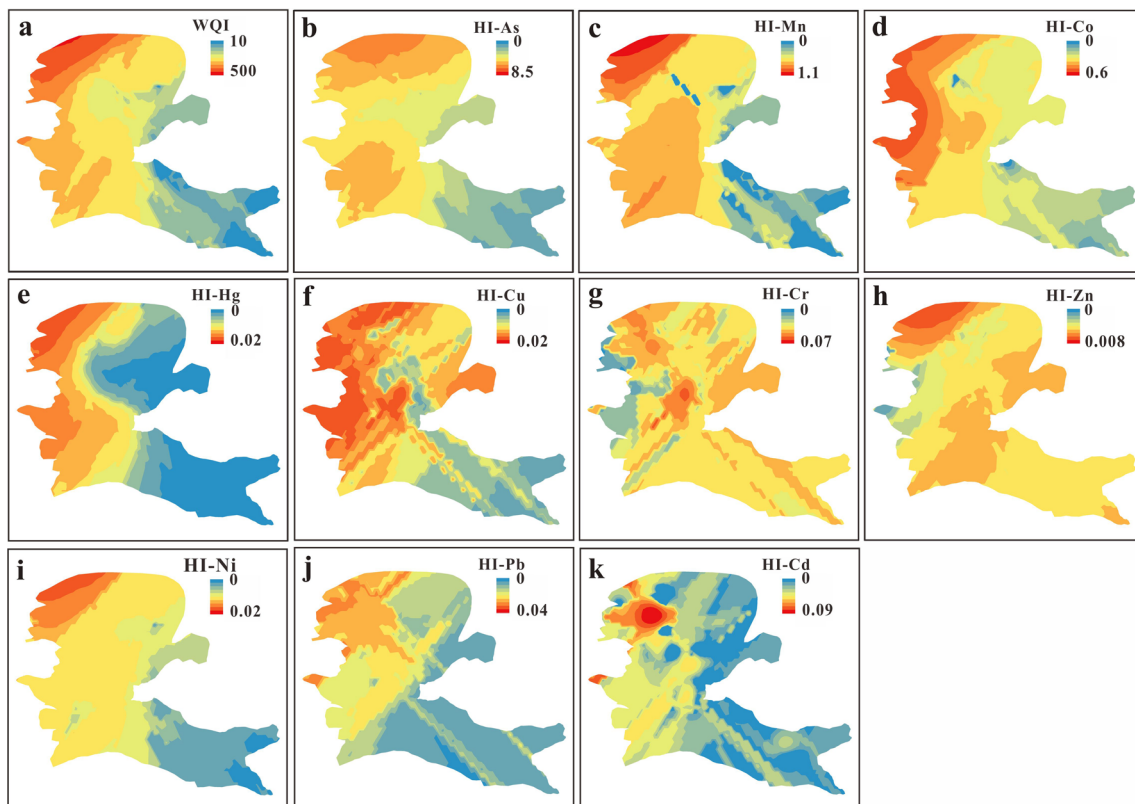


Fig. 8 Spatial variations in the WQI (a) and HI (b–k) values for surface waters in the ADD

et al. 2006; Papa et al. 2004). In addition, displacement of the shoreline and the associated decline in groundwater level prevent exchange of surface water and groundwater, which intensifies evaporation and causes further deterioration of water quality in the flat areas of the ADD (Shibuo et al. 2006; Vitola et al. 2012). The combination of geographic location, climate, and hydrological conditions makes the water along the shoreline the most seriously polluted water in the entire study area. In addition, discharges of industrial and domestic wastewater also have a negative effect on water quality. Inefficient irrigation is a prominent problem in the study area, which not only wastes water, but also contributes to pollution of the aquatic environment. Therefore, it is imperative that better irrigation methods be implemented and that irrigation equipment be updated and maintained. Furthermore, the government can encourage residents to conserve water resources and establish policies to reduce sewage discharge.

Conclusions

Uzbekistan, especially the ADD region near the Aral Sea, has suffered from water volume loss and water quality degradation, which have caused serious environmental problems. We investigated the hydrochemistry and distribution of trace elements in surface waters of the ADBU, to determine the factors that influence element concentrations in surface waters, assess water quality, and evaluate the potability of water throughout the ADBU. We arrived at several important conclusions:

- (i) Surface waters in the ADD are slightly alkaline, and the average TDS value was 1,332 mg/L, much higher than the mean value in the ZR (322 mg/L) and in the world's large rivers. Compared with the ZR region, average concentrations of trace elements in the surface water of the ADD region are relatively high, and As and Mn concentrations in some waters exceed WHO guidelines.
- (ii) Throughout the ADBU, four main hydrochemical types were identified, and they occur in the order $\text{HCO}_3\text{-Ca} < (\text{Cl-Ca}\cdot\text{Mg} + \text{Cl-Na}) < \text{SO}_4\text{-Ca}\cdot\text{Mg}$. The Ca-HCO_3 type only dominated near the mountain pass in the ZR, an area controlled by rock weathering. The hydrochemical type of other river water samples in the ADBU was primarily Ca-Mg-SO_4 , which is controlled by rock weathering and evaporative concentration. Surface waters near the former shoreline in the ADD region and sewage outfalls were dominated by Cl-Ca-Mg and Cl-Na , and reflect the influence of human activities.
- (iii) PCA identified three important factors that account for 86.0% of the total variance in water chemistry. Anthropogenic activities, connected to discharge of industrial wastes, contribute Pb and Cd to the waters.

Higher concentrations of NO_3 , Zn, Ni, Hg, and Mn are related to local agricultural activities. Concentrations of Cu, Cr, As, and Co in surface waters are controlled by both natural processes and human activities.

- (iv) WQI and HQ/HI results show that the worst water quality and the highest degree of potential human health risk exist near the former shoreline in the ADD region. These indices highlight the potential adverse effects on the aquatic environment near the former shoreline in the ADD region, which come from the combination of geographic location, climate, and hydrological conditions. Arsenic has the greatest potential for negatively impacting the health of local residents in the ADBU. Therefore, taking steps to reduce discharge of As into the environment, and to remediate this element where it is present at high concentrations, is of utmost importance.

Supplementary Information The online version contains supplementary material available at <https://doi.org/10.1007/s11356-021-15799-x>.

Acknowledgements We thank the CAS Research Center for Ecology and Environment of Central Asia for assistance with this work, and Huawu Wu and Beibei Shen for field and laboratory assistance. We also thank Mark Brenner for editorial help and three anonymous reviewers for their helpful comments.

Availability of data and materials The data sets supporting the results of this article are included within the article.

Author contribution Shuie Zhan: conceptualization, software, data curation, writing—original draft.

Jinglu Wu: funding acquisition; investigation; writing—review and editing; validation.

Miao Jin: investigation.

Funding The study was supported by the National Natural Science Foundation of China (41671200, and U2003202), and the Strategic Priority Research Program of Chinese Academy of Sciences, Pan-Third Pole Environment Study for a Green Silk Road (XDA2006030101).

Declarations

Ethical approval and consent to participate Not applicable

Consent to publish Not applicable

Competing interests The authors declare no competing interests.

References

- Awan UK, Tischbein B, Martius C (2015) Simulating groundwater dynamics using FEFLOW-3D groundwater model under complex irrigation and drainage network of dryland ecosystems of Central Asia. *Irrig. Drain.* 64:283–296. <https://doi.org/10.1002/ird.1897>

- Chadha DK (1999) A proposed new diagram for geochemical classification of natural waters and interpretation of chemical data. *Hydrogeol J* 7:431–439. <https://doi.org/10.1007/s100400050216>
- Chanpiwat P, Sthiannopkao S (2014) Status of metal levels and their potential sources of contamination in Southeast Asian rivers. *Environ Sci Pollut R* 21:220–233. <https://doi.org/10.1007/s11356-013-1858-8>
- Crosa G, Stefani F, Bianchi C, Fumagalli A (2006) Water security in Uzbekistan: implication of return waters on the Amu Darya water quality. *Environ Sci Pollut R* 13:37–42. <https://doi.org/10.1065/espr2006.01.007>
- Dubovyyk O, Menz G, Conrad C, Kan E, Machwitz M, Khamzina A (2013) Spatio-temporal analyses of cropland degradation in the irrigated lowlands of Uzbekistan using remote-sensing and logistic regression modeling. *Environ Monit Assess* 185:4775–4790. <https://doi.org/10.1007/s10661-012-2904-6>
- Egamberdiyeva D, Mamiev M, Poberejskaya SK (2001) The influence of mineral fertilizer combined with a nitrification inhibitor on microbial populations and activities in calcareous Uzbekistanian soil under cotton cultivation. *Sci World J* 1(S2):108–113. <https://doi.org/10.1100/tsw.2001.301>
- Gaillardet J, Dupre B, Louvat P, Allegre CJ (1999) Global silicate weathering and CO₂ consumption rates deduced from the chemistry of large rivers. *Chem Geol* 159:3–30. [https://doi.org/10.1016/S0009-2541\(99\)00031-5](https://doi.org/10.1016/S0009-2541(99)00031-5)
- Gaillardet J, Viers J, Dupré B (2005) Trace elements in river waters. *Surface and Ground Water, Weathering, and Soils* 5:225–272. <https://doi.org/10.1016/B0-08-043751-6/05165-3>
- Gibbs RJ (1970) Mechanisms controlling world water chemistry. *Science* 170:1088–1090. <https://doi.org/10.1126/science.170.3962.1088>
- Glantz M (1999) *Creeping environmental problems and sustainable development in the Aral Sea Basin*. Cambridge University Press. <https://doi.org/10.1017/CBO9780511535970>
- Graham NT, Hejazi MI, Kim SH, Davies EGR, Edmonds JA, Miralles-Wilhelm F (2020) Future changes in the trading of virtual water. *Nat Commun* 11:3632. <https://doi.org/10.1038/s41467-020-17400-4>
- Habib MA, Islam AMT, Bodrud-Doza M, Mukta FA, Khan R, Siddique MA, Phoungthong K, Techato K (2020) Simultaneous appraisals of pathway and probable health risk associated with trace metals contamination in groundwater from Barapukuria coal basin, Bangladesh. *Chemosphere* 242:125183. <https://doi.org/10.1016/j.chemosphere.2019.125183>
- Han GL, Liu CQ (2004) Water geochemistry controlled by carbonate dissolution: a study of the river waters draining karst-dominated terrain, Guizhou Province, China. *Chem Geol* 204:1–21. <https://doi.org/10.1016/j.chemgeo.2003.09.009>
- Islam AMT, Islam HMT, Mia MU, Khan R, Habib MA, Bodrud-Doza M, Siddique MA, Chu RH (2020) Co-distribution, possible origins, status and potential health risk of trace elements in surface water sources from six major river basins, Bangladesh. *Chemosphere* 249:126180. <https://doi.org/10.1016/j.chemosphere.2020.126180>
- Jalilov SM, Amer SA, Ward FA (2018) Managing the water-energy-food nexus: Opportunities in Central Asia. *J Hydrol* 557:407–425. <https://doi.org/10.1016/j.jhydrol.2017.12.040>
- Khanday SA, Bhat SU, Islam ST, Sabha I (2021) Identifying lithogenic and anthropogenic factors responsible for spatio-seasonal patterns and quality evaluation of snow melt waters of the River Jhelum Basin in Kashmir Himalaya. *Catena* 196:104853. <https://doi.org/10.1016/j.catena.2020.104853>
- Kundzewicz ZW, Kowalczak P (2009) The potential for water conflict is on the increase. *Nature* 459:31–31. <https://doi.org/10.1038/459031a>
- Li PY, He S, Yang NN, Xiang G (2018) Groundwater quality assessment for domestic and agricultural purposes in Yan'an City, northwest China: implications to sustainable groundwater quality management on the Loess Plateau. *Environ Earth Sci* 77:775. <https://doi.org/10.1007/s12665-018-7968-3>
- Micklin P (2007) The Aral Sea disaster. *Annu Rev Earth Planet Sci* 35:47–72. <https://doi.org/10.1146/annurev.earth.35.031306.140120>
- Mirshadiev M, Fleskens L, van Dam J, Pulatov A (2018) Scoping of promising land management and water use practices in the dry areas of Uzbekistan. *Agric Water Manag* 207:15–25. <https://doi.org/10.1016/j.agwat.2018.05.015>
- Njuguna SM, Onyango JA, Githaiga KB, Gituru RW, Yan X (2020) Application of multivariate statistical analysis and water quality index in health risk assessment by domestic use of river water. Case study of Tana River in Kenya. *Process Saf Environ Prot* 133:149–158. <https://doi.org/10.1016/j.psep.2019.11.006>
- Papa E, Castiglioni S, Gramatica P, Nikolayenko V, Kayumov O, Calamari D (2004) Screening the leaching tendency of pesticides applied in the Amu Darya Basin (Uzbekistan). *Water Res* 38:3485–3494. <https://doi.org/10.1016/j.watres.2004.04.053>
- Raj D, Shaji E (2017) Fluoride contamination in groundwater resources of Alleppey, southern India. *Geosci Front* 8:117–124. <https://doi.org/10.1016/j.gsf.2016.01.002>
- Ren X, Li P, He X, Su F, Elumalai V (2021) Hydrogeochemical processes affecting groundwater chemistry in the Central Part of the Guanzhong Basin, China. *Arch Environ Contam Toxicol* 80:74–91. <https://doi.org/10.1007/s00244-020-00772-5>
- Rezaei A, Hassani H, Hassani S, Jabbari N, Fard Mousavi SB, Rezaei S (2019) Evaluation of groundwater quality and heavy metal pollution indices in Bazman Basin, Southeastern Iran. *Groundw. Sustain. Dev.* 9:100245. <https://doi.org/10.1016/j.gsd.2019.100245>
- Rezaei A, Hassani H, Tziritis E, Fard Mousavi SB, Jabbari N (2020) Hydrochemical characterization and evaluation of groundwater quality in Dalgan basin, SE Iran. *Groundw. Sustain Dev* 10:100353. <https://doi.org/10.1016/j.gsd.2020.100353>
- Schettler G, Oberhänsli H, Stulina G, Mavlonov AA, Naumann R (2013) Hydrochemical water evolution in the Aral Sea Basin. Part I: unconfined groundwater of the Amu Darya Delta-Interactions with surface waters. *J. Hydrol.* 495:267–284. <https://doi.org/10.1016/j.jhydrol.2013.03.044>
- Schiermeier Q (2001) Ecologists plot to turn the tide for shrinking lake. *Nature* 412:756–756. <https://doi.org/10.1038/35090704>
- Shibuo Y, Jarsjo J, Destouni G (2006) Bathymetry-topography effects on saltwater-fresh groundwater interactions around the shrinking Aral Sea. *Water Resour Res* 42:W11410. <https://doi.org/10.1029/2005WR004207>
- Tornqvist R, Jarsjo J, Karimov B (2011) Health risks from large-scale water pollution: trends in Central Asia. *Environ Int.* 37:435–442. <https://doi.org/10.1016/j.envint.2010.11.006>
- UENP (2016) Third National Communication of the republic of Uzbekistan under the UN Framework Convention on Climate Change. Available from: https://unfccc.int/sites/default/files/resource/TNC%20of%20Uzbekistan%20under%20UNFCCC_english_n.pdf. Accessed 9 Aug 2021
- USEPA (2004) Risk Assessment Guidance for Superfund Volume 1. Human Health Evaluation Manual (Part E, Supplemental Guidance for Dermal Risk Assessment). Available from: https://www.epa.gov/sites/default/files/2015-09/documents/part_e_final_revision_10-03-07.pdf. Accessed 9 Aug 2021
- USEPA (2010) Regional Screening Level (RSL) tapwater supporting table. Available from: https://epa-prgs.ornl.gov/chemicals/download/master_sl_table_run_JUN2011.pdf. Accessed 9 Aug 2021
- Vitola I, Vircavs V, Abramenko K, Lauva D, Veinbergs A (2012) Precipitation and air temperature impact on seasonal variations of groundwater levels. *Environ Clim Technol* 10:25–33. <https://doi.org/10.2478/v10145-012-0022-x>
- Wang XL, Luo Y, Sun L, He CS, Zhang YQ, Liu SY (2016) Attribution of runoff decline in the Amu Darya River in Central Asia during 1951–2007. *J Hydrometeorol* 17:1543–1560. <https://doi.org/10.1175/JHM-D-15-0114.1>

- Wang J, Liu GJ, Liu HQ, Lam PKS (2017) Multivariate statistical evaluation of dissolved trace elements and a water quality assessment in the middle reaches of Huaihe River, Anhui, China. *Sci Total Environ* 583:421–431. <https://doi.org/10.1016/j.scitotenv.2017.01.088>
- Wei MJ, Wu JH, Li WQ, Zhang QX, Su FM, Wang YH (2021) Groundwater geochemistry and its impacts on groundwater arsenic enrichment, variation, and health risks in Yongning County, Yinchuan Plain of northwest China. *Expos. Health* 1–20. <https://doi.org/10.1007/s12403-021-00391-y>
- WHO (World Health Organization) (2011) Guidelines for drinking water quality, fourth ed. Available from: http://apps.who.int/iris/bitstream/handle/10665/44584/9789241548151_eng.pdf;sequence=1. Accessed 9 Aug 2021
- Wu HW, Wu JL, Li J, Fu CS (2020) Spatial variations of hydrochemistry and stable isotopes in mountainous river water from the Central Asian headwaters of the Tajikistan Pamirs. *Catena* 193:104639. <https://doi.org/10.1016/j.catena.2020.104639>
- Yang XW, Wang NL, Chen AA, He J, Hua T, Qie YF (2020) Changes in area and water volume of the Aral Sea in the arid Central Asia over the period of 1960-2018 and their causes. *Catena* 191:104566. <https://doi.org/10.1016/j.catena.2020.104566>
- Zeng XX, Liu YG, You SH, Zeng GM, Tan XF, Hu XJ, Hu X, Huang L, Li F (2015) Spatial distribution, health risk assessment and statistical source identification of the trace elements in surface water from the Xiangjiang River, China. *Environ Sci Pollut R* 22:9400–9412. <https://doi.org/10.1007/s11356-014-4064-4>
- Zhan SE, Wu JL, Wang JZ, Jing M (2020) Distribution characteristics, sources identification and risk assessment of n-alkanes and heavy metals in surface sediments, Tajikistan, Central Asia. *Sci Total Environ* 709:136278. <https://doi.org/10.1016/j.scitotenv.2019.136278>

Publisher's note Springer Nature remains neutral with regard to jurisdictional claims in published maps and institutional affiliations.